Kinetics and Fixed-Bed Reactor Modeling of Butane Oxidation to Maleic Anhydride

Ramesh K. Sharma and David L. Cresswell
Systems Engineering Group, Federal Institute of Technology, CH-8092 Zürich, Switzerland

Esmond J. Newson
Swiss Aluminium R&D, CH-8212 Neuhausen, Switzerland

Selective oxidation kinetics of n-butane to maleic anhydride in air were studied over a commercial, fixed-bed vanadium-phosphor oxide catalyst. The temperature range was 573-653 K with butane concentrations up to 3 mol % in the feed, which is within flammability limits but below ignition temperatures.

The rate data were modeled using power law kinetics with product inhibition and included total oxidation and decomposition reactions. Kinetic parameters were estimated using a multiresponse, nonlinear regression algorithm showing intercorrelation effects. The kinetics were combined with independent measurements of catalyst diffusivity and reactor heat transfer using a one-dimensional heterogeneous reactor model. Model predictions and observed temperatures and concentrations from nonisothermal pilot plants were compared up to 115 days on stream. Agreement was acceptable with inlet butane concentrations up to 2.7 mol %. For example, runaway was predicted at a salt temperature 3 K higher than observed. Effectiveness factors around the hot spot were estimated at 0.6 with the catalyst surface temperature 2-3 K higher than the average gas temperature.

Introduction

For economic and ecological reasons, *n*-butane is replacing benzene as the major feedstock for the production of maleic anhydride. Enhanced catalyst activity and selectivity (Budi et al., 1982), together with anhydrous, organic solvent absorption downstream (Neri and Sanchioni, 1982), make the economics for the fixed-, or fluidized-bed process exbutane particularly favorable. More recently, a recirculating solids reactor has been described, which optimizes the best features of fixed and fluidized beds (Contractor et al., 1988).

Whatever the preferred technology, knowledge of the intrinsic kinetics is essential for optimizing the reactor design (Schneider et al., 1987; Wellauer et al., 1986). For safety in reactor operation with respect to temperature runaway at high butane inlet concentrations, a study has been made (Sharma et al., 1984b), whose kinetics were used for comparison of runaway situations in commercial pilot-plant reactors.

Prior kinetic studies have been undertaken from either of two experimental viewpoints. The first and more fundamental approach is the identification of intermediate surface species and their relative concentrations to understand the reaction mechanism and different reaction pathways (Centi et al., 1988; Hodnett, 1987; Wenig and Schrader, 1986). Many such publications, however, fail to quantify kinetics for subsequent reaction engineering and reactor optimization. The alternate approach is to obtain intrinsic reaction data, which is then confronted with different empirical and mechanistic models (Centi et al., 1985). This approach requires statistical interpretation of the data to discriminate among different models and to show intercorrelation of parameters thus selecting the most probable kinetic parameters (Schneider et al., 1987; Sharma et al., 1984b).

The latter approach was chosen for this work whose purpose is to develop an intrinsic kinetic model, which is not only consistent with laboratory and pilot-plant kinetic measurements but also capable of being combined with heat and mass

Correspondence concerning this article should be addressed to E. J. Newson, Paul Scherrer Institute, Dept. F5, CH-5232 Villigen PSI, Switzerland.

Present address: R. K. Sharma, Dept. of Chemical Engineering, University of Saskatchewan, Saskatoon, Canada, S7N 0W0; D. L. Cresswell, Chemicals and Polymers Ltd., P.O. Box 8, The Heath, Runcorn, Cheshire, England, WA7 4QD.

transport steps to predict nonisothermal, fixed bed, pilot-plant data at commercial conditions. The kinetic work was accomplished in three stages first using isothermal, differential rate data, then isothermal integral rate data from pilot plants, and finally testing the scale-up properties of the reactor model against full-scale pilot-plant data.

The major results of this work are based on kinetic data with an industrial catalyst at high (≤ 3 mol %) inlet butane concentrations in the temperature range 573–653 K. Only data from isothermal, integral pilot plants 1:1 with commercial reactors and on equilibrated catalyst were used in the final analyses, the latter point being rarely conceded as important in the literature (Centi et al., 1988; Schneider et al., 1987). Data from laboratory reactors proved quite misleading in establishing the final triangular kinetic scheme with product inhibition. This surprising result was independently confirmed (Buchanan, 1985). The temperature and concentration measurements along the length of the pilot-plant reactor were crucial for satisfactory parameter estimation, in addition to the presence of maleic anhydride at the inlet to the test section of the reactor to avoid systematic errors.

For rigorous testing of the kinetic and reactor models, predictions were compared with data from full-scale pilot-plant reactors operated near stability limits. The effects of salt temperature, inlet butane concentration and feed rate were illustrated up to runaway conditions. The heterogeneity of the model indicated effectiveness factors for the catalyst of about 0.6 at the hot spot, but little difference between catalyst and average gas temperatures.

The Reactor Model

An appropriate compromise between excessive complexity and oversimplification for such highly exothermic fast reactions is a one-dimensional, heterogeneous model (Froment, 1972). The utility of such a model has been shown for the vapor-phase oxidation of benzene to maleic anhydride (Sharma et al., 1984a). The effects of axial and radial dispersion of heat and mass can be neglected as a first approximation, since they are relevant only over a short length of the industrial reactor in the region of the hot spot.

Reaction network

A simplified reaction network consistent with the literature and preliminary work is a triangular kinetic model with the desired reaction of butane to maleic anhydride in parallel with an undesired, total oxidation reaction. The decomposition reaction of maleic anhydride to oxidation products closes the network. The stoichiometric equations are:

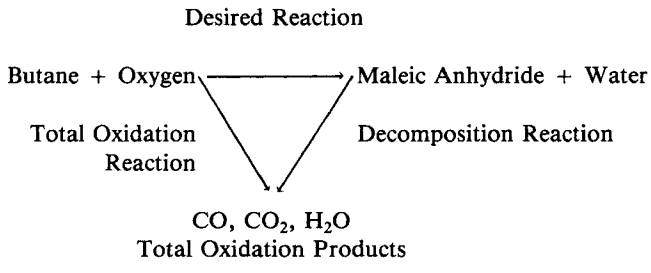

$$C_4H_{10} + 3.5O_2 \rightarrow C_4H_2O_3 + 4H_2O \quad (1)$$

$$C_4H_2O_3 + pO_2 \rightarrow (6-2p)CO + (2p-2)CO_2 + H_2O \quad (2)$$

$$C_4H_{10} + nO_2 \rightarrow (13-2n)CO + (2n-9)CO_2 + 5H_2O \quad (3)$$

p and n are stoichiometric coefficients dependent on the catalyst and are determined by kinetic measurements.

Reactor equations

Mass balance:

$$\frac{G_m}{(1-\epsilon)M}\frac{dp_i}{dZ} = \sum_{j=1}^{3} a_{ij}\eta(j)R(j) \quad (4)$$

Energy balance:

$$G_m C_p \frac{dT}{dZ} = \sum_{j=1}^{3} (-\Delta H_j)\eta(j)R(j)(1-\epsilon) - U_{ov}\cdot A\cdot(T-Ts) \quad (5)$$

where $\eta(j)$ and $R(j)$ are the effectiveness factor and reaction rate, respectively, for the jth reaction and a_{ij} is the stoichiometric number for the ith species in jth reaction, which is positive for product and negative for the reactant. The pressure drop across the reactor was calculated using the Ergun equation (Ergun, 1952).

Pellet equations:

$$\frac{1}{r^a}\frac{d}{dr}\left(D_{\text{eff}i}\, r^a \frac{dC_i}{dr}\right) = \sum_{j=1}^{3} -a_{ij}R(j) \quad (6)$$

$$\frac{1}{r^a}\frac{d}{dr}\left(K_{\text{eff}}\, r^a \frac{dT}{dr}\right) = \sum_{j=1}^{3} -(-\Delta H_j)R(j) \quad (7)$$

Boundary conditions:

$$r = 0, \frac{dT}{dr} = \frac{dCi}{dr} = 0 \quad (8)$$

$$r = b, C_i = C_{io} - \frac{b}{Bi_m}\frac{dCi}{dr} \quad (9)$$

$$T = T_o - \frac{b}{Bi_h}\frac{dT}{dr} \quad (10)$$

$$Bi_m = \frac{k_g b}{D_{\text{eff}}} \text{ and } Bi_h = \frac{hb}{K_{\text{eff}}} \quad (11)$$

The feed entrance conditions to the reactor are known. Such equations need to be written only for butane, oxygen, and maleic anhydride. The corresponding concentrations for CO, CO_2, and H_2O can be calculated from reaction stoichiometry and rates. Using a modified Euler predictor-corrector method, the interstitial fluid-phase equations were integrated stepwise starting at the reactor inlet in conjunction with the pellet equations employing two corrections for optimal usage and a step

Table 1. Heat transfer Parameters for Butane Oxidation to Maleic Anhydride

$k_{r,\text{eff}}$	$= 1.1\ \text{W}\cdot\text{m}^{-1}\cdot\text{K}^{-1}$
$h_{w,\text{eff}}$	$= 164\text{-}167\ \text{W}\cdot\text{m}^{-2}\cdot\text{K}^{-1}$
(Bed + inside wall) coefficient	$= 111\text{-}113\ \text{W}\cdot\text{m}^{-2}\cdot\text{K}^{-1}$
Overall heat transfer coefficient (U_{ov})	$= 105\text{-}107\ \text{W}\cdot\text{m}^{-2}\cdot\text{K}^{-1}$
Biot number for heat	= 0.66-0.67

size of 2 cm (Seinfeld and Lapidus, 1974). The coupled set of two-point boundary value equations describing the pellet were solved by orthogonal collocation using Jacobi polynomials as expansion functions (Villadsen and Michelsen, 1978). Computation time for a 3-m-long reactor was about 65 s on a CDC 6400 computer. The effectiveness factors $\eta(j)$ for any reaction are computed from the reaction rates integrated over the catalyst pellet:

$$\eta(j) = \frac{(a+1)\int_o^b r^a \cdot R(j)\cdot dr}{b^{a+1}R(j)\,(T_G, p_G)} \tag{12}$$

where a is a geometry factor and equal to 0, 1, and 2 for a slab, infinite cylinder, and sphere, respectively.

Heat transfer in the reactor tube

This has been described by a two-phase continuum model based on a diffusional model for heat transfer that allows for different temperature profiles in solid and fluid phases and includes axial conduction in both the fluid and solid (Wellauer et al., 1982). The overall heat transfer coefficient is based on the measured temperature difference between the central axis of the bed and the coolant. It is derived by asymptotic matching of thermal fluxes between one-dimensional and two-dimensional models using the effective radial thermal conductivity, $k_{r,\text{eff}}$, and the wall heat transfer coefficient, $h_{w,\text{eff}}$. According to the model, the overall heat transfer coefficient U_{ov} can be calculated by:

$$U_{ov} = h_{w,\text{eff}} J_o\ (\alpha_1) \tag{13}$$

where α_1 is the smallest root of

$$\alpha J_1(\alpha) = \frac{h_{w,\text{eff}} d_t}{2k_{r,\text{eff}}} \cdot J_o(\alpha) \tag{14}$$

J_o is a zero-order Bessel function of the real kind. Table 1 shows typical values of these parameters for one set of experimental data from a full-scale pilot plant.

Local heat and mass transfer parameters

These parameters are essential to calculate surface conditions from measurable gas-phase temperatures and concentrations. The fluid-solid heat transfer coefficient is calculated from the relation (Dwivedi and Upadhyay, 1977)

$$Nu = \frac{hdp}{k_{gs}} \tag{15}$$

$$= \frac{0.57}{\epsilon} Pr^{1/3} Re_p^{0.6}\ Re_p \geq 50 \tag{16}$$

where Nu is the Nusselt number. The corresponding mass transfer coefficient can be calculated from the heat and mass transfer analogy assuming Prandtl and Schmidt numbers for air to be equal. Typical ratios for inter- and intraparticle transport rates are 0.66 for heat and 250 for mass.

Kinetic model for butane oxidation to maleic anhydride

Two types of mechanistic models were considered to describe the triangular kinetics for the selective oxidation of butane, i.e., Langmuir-Hinshelwood and Redox mechanisms. Since alternative kinetic data on a fluidized-bed catalyst of the same composition showed that, above 15% oxygen in the feed, the reaction rates were independent of oxygen concentration for butane conversions up to 70%, the rate equations could be simplified. Preliminary work in an isothermal integral reactor had also shown that a maleic anhydride adsorption term was required to better describe concentration profiles in the reactor. The rate equations for the best model were:

$$R_1 = \frac{k_1 p_1^{\alpha 1}}{(1+K_2 p_2)} \quad \text{desired reaction} \tag{17}$$

$$R_2 = \frac{k_2 p_2}{(1+K_2 p_2)^2} \quad \text{decomposition reaction} \tag{18}$$

$$R_3 = k_3 p_1^{\alpha 3} \quad \text{total oxidation reaction} \tag{19}$$

To minimize correlation, the rate constants were reparameterized as

$$k_{jT} = k_{j673}\exp\left[\frac{E_j}{673\text{R}}\left(1 - \frac{673}{T}\right)\right] \tag{20}$$

where k_{j673} is the value of the rate constant k_j at the reference temperature of 673 K.

Interpretation of the isothermal data

Using the integral method of data analysis, the triangular kinetics leads to the following equations for the system under isothermal conditions and assuming constant density and constant number of moles

$$\frac{dp_1}{dZ} = \frac{(1-\epsilon)}{F_t}\Omega\ (R_1+R_2) \tag{21}$$

$$\frac{dp_2}{dZ} = \frac{(1-\epsilon)}{F_t}\Omega\ (R_1-R_2) \tag{22}$$

$$\frac{dp_3}{dZ} = \frac{(1-\epsilon)\Omega}{F_t}[(2p-2)R_2 + (2n-9)R_3] \tag{23}$$

$$\frac{dp_4}{dZ} = \frac{(1-\epsilon)\Omega}{F_t}[(6-2p)R_2 + (13-2n)R_3] \tag{24}$$

where

$p_1, \cdots p_4$ = dimensionless partial pressures of n-butane, maleic anhydride, carbon dioxide and carbon monoxide, respectively

Z = axial bed length
Ω = cross-sectional reactor area
ϵ = bed voidage

For given rate models, the above equations were integrated numerically and fitted to observed reactant-product distributions employing the nonlinear regression program of Klaus and Rippin (1979) utilizing a Marquardt routine. Basic assumptions in the program are that there are no systematic deviations between the model and the physical system, the residuals are only due to errors in the measured responses p_1 to p_4, and the errors between different experiments are not correlated. Allowance is made, however, for correlation between measured responses in any single run. Initial estimates of the parameters were obtained from graphical testing of the data. The objective function S was minimized with respect to the parameters $\underline{\theta}$ where

$$S = \frac{1}{2} \sum_{f=1}^{\ell} n_f \sum_{g=1}^{mf} \ln [M_f(\theta)] \tag{25}$$

where m_f is the number of responses in pattern f, n_f is the number of measurements in pattern f, ℓ is the number of different patterns and $M_f(\underline{\theta})$ is the determinant of the $(M_f \times m_f)$ moment matrix of residuals of pattern f. The convergence criterion for each parameter was 1×10^{-4}.

Diffusion inside the catalyst

The effective diffusivity of the catalyst was calculated by combining Knudsen and bulk diffusion contributions in the Bosanquet relation (Satterfield, 1970).

$$\frac{1}{D_{\text{eff}}} = \frac{1}{D_{K,\text{eff}}} + \frac{1}{D_{B,\text{eff}}} \tag{26}$$

where

$$D_{B,\text{eff}} = D_B \frac{E_p}{\tau} \frac{1}{P} \left(\frac{T}{T_{ref}}\right)^{1.5} \tag{27}$$

$$D_{K,\text{eff}} = 9{,}700\, \bar{r} \frac{E_p}{\tau} \left(\frac{T}{M}\right)^{0.5} \tag{28}$$

The tortuosity factor τ was measured experimentally, $\bar{r}$ is the mean pore radius in cm.

Experimental Studies

The catalyst consisted of promoted vanadium-phosphor oxides whose commercial form is 3×10^{-3}-m-dia. extrudates. The pore-size distribution by mercury porosimetry showed pores in the range 10^{-8}–10^{-6} m diameter, a pore volume of 0.38×10^{-9} m^3·kg^{-1}, and a BET surface area of 11×10^{-3} m^2·kg^{-1}.

Measurement of the tortuosity factor

A single-pellet string column was used to measure the tortuosity under nonreacting conditions by pulse broadening (Cresswell and Orr, 1982). Nitrogen and helium were used as tracer gases. Since pulse broadening can also be caused by axial dispersion in addition to pore diffusion, the former was measured independently using identical nonporous glass particles. Table 2 shows the results of the experiments. An average tortuosity of 3 was used for all the species of the reaction mixture, since the molecular weight of nitrogen is closer to butane than helium.

Table 2. Tortuosity Factor for Butane Oxidation Catalyst

Reynolds No. (Re_p)	Peclet No. (Pe_p)	Effective Diffusivity m^2·s^{-1}($\times 10^6$)	Tortuosity Factor τ
Nitrogen Pulse			
62.2	1.88	1.99	3.3
50.1	1.93	2.15	3.0
40.8	1.99	2.18	3.0
28.4	2.12	2.53	2.6
19.5	2.31	2.06	3.2
10.7	2.77	2.09	3.1
Helium Pulse			
399.9	1.92	2.90	4.9
363.2	1.94	2.61	5.1
274.6	2.03	2.72	4.8

Reactor systems used

Kinetic parameters were estimated from experiments carried out in isothermal differential and integral reactors both with crushed and commercial extrudate sizes. The overall experimental program is described in Table 3. The diluted bed integral reactor data, from which the kinetic parameters were ultimately determined, were fractional in design including four temperature levels, four concentration levels, and three flow rates. In a series of 40 experiments, a total of 160 points were observed, and at each point the concentrations of four species were measured. The total of 640 data points were considered sufficient to estimate the minimum expected six-parameter model.

Table 3. Scope of Experiments: Butane Kinetics and Nonisothermal Operation

	Isothermal		Nonisothermal
	Laboratory Differential	Pilot-Plant Low/High Conversion	Pilot-Plant High Conversion
Total pres., atm	1.1	1–3	1–3
Salt temp., °C	300–370	320–380	360–400
Total feed rate kmol$\times 10^{-3}$h^{-1}	1–3	50–240	40–80
Mole fraction (inlet)			
C_4H_{10}	0.005–0.03	0.005–0.03	0.018–0.027
O_2	0.21	0.21	0.21
$C_4H_2O_3$	0	0.001–0.002	0
Cat. particle size, mm	0.7, 7	3	3
Cat. weight, g	1–3	600–740	1,800–2,280

The differential reactor was a 60-cm-long, 35-mm-dia. glass tube placed in an electrically heated furnace. The temperature in the reactor bed was measured by a sliding chrome-alumel thermocouple placed in an axial thermowell. Dilution of the catalyst with glass beads of the same size in the ratio 1:9 practically gave isothermal conditions, the temperature variation along the length of the reactor not exceeding 2°C. Butane conversions did not exceed 8%. Under conditions chosen for the differential reactor, calculations for interphase transport limitations (Gunn, 1978) showed that mass transfer rates were at least 100 times larger than reaction rates, and gas-solid temperature differences were a maximum of 2°C.

To check the role of product inhibition on kinetics, liquid maleic anhydride was pumped to the inlets of both differential and integral reactors. Practically this proved so difficult that experiments were carried out only with diluted-bed integral reactors to emphasize kinetic measurements in the presence of maleic anhydride. In initial work, 3-mm commercial-size extrudates were packed in a 4-m-long, 25-mm-ID reactor tube immersed in a stirred molten saltbath for cooling. The tube had several intermediate sampling points and an axial thermowell for temperature measurements. In the front 40% of the reactor, an inert to catalyst ratio of 1:2 was used, concentration measurements were made only in the second section of the reactor. In a more extensive work using up to 3 mol % inlet butane, catalyst dilution was used in both sections: 1:1 in the front and 1:0.5 (inert) downstream.

The product analyses were performed in the same way as the differential reactor experiments. Maleic anhydride in the product gases was absorbed in water and titrated against a standard alkali solution. Butane concentrations at the inlet and outlet were measured using gas chromatography, and CO and CO_2 were analyzed by an infrared instrument. Any runs with a carbon balance not within ±3% were rejected.

Safety aspects of reactor operation

The high inlet butane concentrations in air used in this work were often between the upper and lower flammability limits of 10.3 and 1.7% by volume, respectively (Perry et al., 1963). The spontaneous ignition temperature at the stoichiometric concentration of 3.1% is 704 K, which increases to about 820 K at 1.7%. Thus salt-bath temperatures of 673 K were not exceeded in this work for safety reasons.

To further ensure safe operation if flammability limits and ignition temperatures were simultaneously reached, standard procedures for such laboratories were additionally used. Rupture discs at the top of the reactor are large and quick enough to act to mitigate emergencies, automatic hydrocarbon feed shut off with nitrogen purge for variations of pressure and temperature outside predefined limits, visual and audible alarm facilities.

The possibility of flame propagation in the fixed catalyst bed is minimal due to the packing acting as a flame arrestor. In the equipment before the packing where the greatest danger lies, entering hydrocarbon/air mixtures are preheated only to about 450 K, well below the spontaneous ignition temperature. Thus, the first few centimeters of catalyst are used to bring the feed up to reaction temperatures, but safely inside the packed bed. In equipment after the packing, temperatures drop sharply, while exit concentrations of butane are well below flammability limits in high conversion operation.

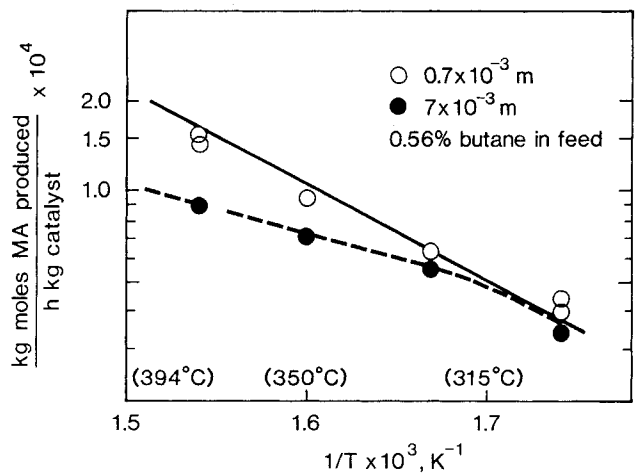

Figure 1. Influence of pore diffusion on reaction rate.

Results and Discussion

To study intraparticle diffusion, experiments were carried out in the differential reactor with 7×10^{-3}-m and 0.7×10^{-3}-m-dia. catalyst pellets. The observed rates are shown in Figure 1 indicating that pore diffusion is significant above 653 K. Isothermal, integral reactor experiments were, therefore, performed with 3×10^{-3}-m-dia. extrudates operating below 653 K.

Kinetic parameters from the differential reactor

Since conversions were small and the inlet concentration of maleic anhydride was zero, the rate data were first modeled assuming two parallel reactions following power law rate

Table 4. Four-Parameter Simplified Model for Butane Kinetics: Differential Reactor

$k_1 = (0.94 \pm 0.73)10^{-6}\text{kmol}\cdot\text{kg}^{-1}\cdot\text{s}^{-1}\cdot\text{atm}^{0.66}$
$E_1 = E_3 = 63{,}600 \pm 13{,}800\ \text{kJ}\cdot\text{kmol}^{-1}$
$\alpha_1 = \alpha_3 = 0.66 \pm 0.16$
$k_3 = (0.40 \pm 0.32)10^{-6}\text{kmol}\cdot\text{kg}^{-1}\cdot\text{s}^{-1}\cdot\text{atm}^{0.66}$

Correlation Matrix

k_1	1.00			
E_1	0.48	1.00		
k_3	0.97	0.47	1.00	
α_1	0.99	0.53	−0.97	1.00

Objective Function Value = −288

$\left(\frac{\sigma}{r}\right)_1^* = 30.3\%$ $\left(\frac{\sigma}{r}\right)_2 = 9.6\%$

$\left(\frac{\sigma}{r}\right)_3 = 24.2\%$ $\left(\frac{\sigma}{r}\right)_4 = 15.9\%$

Stoichiometric Coefficient: n = 5.5

* = (standard deviation of residuals of fitted response/range of response) × 100
1 = butane; 2 = maleic anhydride; 3 = CO_2; 4 = CO
± = 95% confidence limits

expressions. This six-parameter model showed that k_3 and α_3 were poorly determined and with a strong correlation between rate constant and reaction order. A simplified four-parameter model gave better estimates, which are shown in Table 4 with their single-parameter 95% confidence limits, correlation matrix, objective function value and accuracy of fit. Joint parameter confidence limits are expected to be somewhat larger, about 50%. However, reducing the total number of parameters from six to four did not increase the objective function significantly. Also, k_1 and k_3 are highly correlated as are k_1 and α_1, and k_3 and α_1. The inability to control the maleic anhydride feed to the inlet of the differential reactor probably led to systematic errors accompanying the differential data (Cropley, 1987). The estimate of 63,600 ± 13,800 kJ/kmol^{-1} is about 50% lower than subsequent integral data which included product inhibition at the reactor inlet.

Incorporating the kinetics from Table 4 into the reactor model (Eqs. 4-11) and comparison with experimentally observed temperature and concentration profiles from a 4-m pilot-plant reactor indicated severe discrepancies. Since reaction rates were underpredicted in the front end and overestimated in the tail end of the reactor, the kinetic model was modified to include inhibition by the product maleic anhydride. This is consistent with an *in situ* FTIR study of *n*-butane selective oxidation to maleic anhydride on V-P-O catalysts in which the carbonyl stretching vibrations of maleic acid and maleic anhydride were observed (Wenig and Schrader, 1986).

Kinetic parameters from isothermal integral reactors

The initial integral reactor work in the 4-m tube, with only the front end diluted, was combined with independent measurements of maleic anhydride decomposition kinetics in a laboratory salt-bath reactor (Kuhn, 1979). The latter work led to the use of incorrect stoichiometry $p=2$, $n=5.5$, when applied to full-scale pilot-plant data where CO/CO_2 ratios were always greater then 1.0. The more extensive work using up to 3 mol % inlet butane with catalyst dilution in both sections was, therefore, used to determine all the kinetic parameters including the decomposition reaction. The resulting seven-parameter model, Table 5, gave better estimates, decreased the objective function value, and decreased the % standard deviation in comparison to Table 4. A maleic anhydride adsorption term is now included, and the activation energy of the decomposition reaction, 155 MJ·kmol^{-1} compared to the desired reaction 93.1 MJ·kmol^{-1}, clearly shows the disadvantage with respect

Table 5. Seven-Parameter Model for Butane Kinetics: Isothermal Integral Reactor

$k_1 = (0.96 \pm 0.28)10^{-6}$ kmol·kg^{-1}·s^{-1}·atm$^{0.54}$
$E_1 = E_3 = 93{,}100 \pm 5{,}700$ kJ·mol^{-1}
$\alpha_1 = \alpha_3 = 0.54 \pm 0.05$
$k_2 = (0.29 \pm 0.14)10^{-5}$ kmol·kg^{-1}·s^{-1}·atm^{-1}
$E_2 = 155 \pm 35$ MJ·kmol^{-1}
$k_3 = (0.15 \pm 0.03)10^{-6}$ kmol·g^{-1}·s^{-1}·atm$^{-0.54}$
$K_2 = 310 \pm 125$ atm^{-1}

Correlation Matrix

k_1	1.00					
E_1	0.68	1.00				
k_3	0.87	0.55	1.00			
α_1	0.94	0.62	0.94	1.00		
k_2	0.50	0.46	0.08	0.34	1.00	
E_2	−0.20	−0.31	0.09	−0.13	−0.83	1.00
K_2	0.69	0.63	0.39	0.44	0.61	−0.22 1.00

Objective Function Value = −606

$\left(\frac{\sigma}{r}\right)_1^* = 3.7\%$ $\left(\frac{\sigma}{r}\right)_2 = 3.0\%$

$\left(\frac{\sigma}{r}\right)_3 = 6.8\%$ $\left(\frac{\sigma}{r}\right)_4 = 2.3\%$

Stoichiometric Coefficients: p = 1, n = 5.5

* = (standard deviation of residuals of fitted response/range of response) × 100
1 = butane; 2 = maleic anhydride; 3 = CO_2; 4 = CO
± = 95% confidence limits

Table 6. Testing of the Butane Reactor Model against Pilot-Plant Data

Days On Stream	111	112	113	114	115
Operating Conditions					
Feed rate, m^3·h^{-1}	1.67	1.67	1.27	0.95	0.95
Inlet butane conc., %	1.81	1.81	2.20	2.57	2.68
Salt temperature, °C	383	363	363	363	373
Experimental Data					≥600
Hot spot, °C	420	375	380–85	390–95	Runaway!
Conversion, %	85	60	65	50	60–65
Selectivity*, %	55	67	63	56	—
Model Predictions					Runaway
Hot spot*, °C	422	383	390	401	(Salt temp. = 376°C)
Conversion, %	82.3	58.6	64.4	72.9	92
Selectivity, %	61.1	66.4	63.5	59.3	53
CO/CO_2 ratio	1.48	1.25	1.26	1.27	1.62
Overall heat trans. coeff. U_{ov}, W·m^{-2}·K^{-1}	106	104	93	83	85

*Hot spot refers to axial gas temperature
**selectivity = moles maleic anhydride, ma/mol·ma + mol·(CO + CO_2)/4.

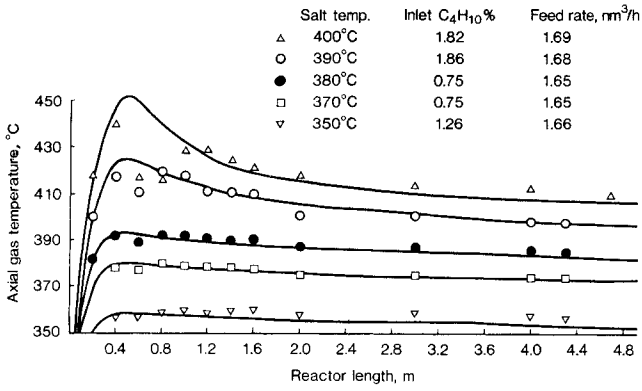

Figure 2. Maleic anhydride exbutane temperature profiles at various operating conditions: experimental catalyst

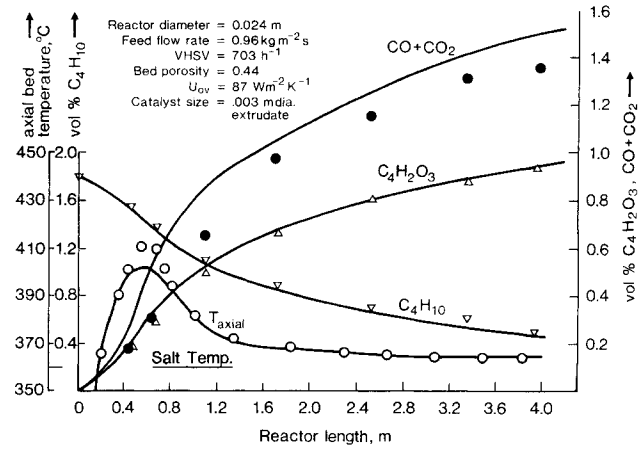

Figure 3. Observed and predicted reactant, product and temperature distributions in a full-scale reactor tube.

to selectivity of operation with high hot spots. A temperature dependence of K_2 could not be estimated with any certainty so it was considered constant.

The relative contribution of reactions 2 and 3 to the formation of CO and CO_2 is reflected in the new values of the stoichiometric coefficients $p=1$, $n=5.5$. These values allow CO/CO_2 ratios greater than 1.0 as frequently seen in nonisothermal operation with hot spots.

Model predictions vs. pilot-plant data

For rigorous testing of the kinetic and reactor model, predictions were compared with data from a full-scale pilot-plant reactor operated near stability limits due to low feed rates and high hydrocarbon concentrations. The reactor was 25-mm-dia, 5-m-long, and fitted with an axial thermowell. The catalyst was very similar to that used for kinetic measurements. Table 6 shows a comparison of model predictions vs. experimental data at different operating conditions. Conversion and selectivity have been calculated at average gas temperatures given by the one-dimensional model while predicted hot-spot temperatures are for the gas at the axial location, using the two-dimensional continuum model of heat transfer, as described earlier. The data from 111, 112 and 113 days on stream indicate that the model satisfactorily predicts the effects of salt temperature, inlet butane concentration, and feed rate. At 114 days on stream, predicted conversion is much higher than observed due possibly to an observed reactor upset since operation was on the verge of stability. Runaway was predicted at a salt temperature 3°C higher than observed at a butane inlet concentration of 2.68%.

In a series of runs, the model was further tested using an experimental catalyst. The temperature profiles at the respective conditions are shown in Figure 2 and the comparison of experimental and predicted exit concentrations are shown in Table 7. For salt temperatures between 350–400°C, Figure 2 shows that temperatures are well predicted. Table 7 shows that conversion and selectivity are satisfactorily predicted especially at higher conversions.

Observed and predicted concentration and temperature profiles in a full-scale reactor tube are shown in Figure 3. The conversion of butane and selectivity to maleic anhydride are well predicted. The hot-spot temperature is underpredicted but within the uncertainty of the heat transfer coefficient (±10%) (Wellauer et al., 1982). The combined CO + CO_2 profile illustrates the relative contributions of reactions 2 and 3 and tests the stoichiometry shown in Table 5, $p=1$, $n=5.5$. The CO/CO_2 ratio at the reactor exit as shown in Table 7 also tests the suitability of the chosen stoichiometry.

Table 7. Testing the Model with Data from an Experimental Catalyst in Pilot-Plant Reactors

Conditions	1	2	3	4	5
Operating Conditions					
Feed rate, $m^3 \cdot h^{-1}$	1.68	1.68	1.65	1.65	1.66
Inlet butane conc., %	1.82	1.86	0.75	0.75	1.26
Salt temperature, °C	400	390	370	380	350
Inlet pressure, atm	1.9	1.65	1.64	1.64	1.62
Experimental/Predicted					
Hot spot, °C	440/451	419/424	380/380	392/393	360/359
Conversion, %	90/90.8	84/77.2	81/72.4	89.4/82.4	52.3/42.2
Selectivity, %	60/57.5	68/63.4	71.9/73.2	66.1/71.2	81.6/74.2
CO/CO_2 ratio	1.51/1.7	1.55/1.49	1.56/1.37	1.57/1.51	1.43/1.16
Pressure drop, atm	0.9/0.6	0.65/0.61	0.64/0.70	0.64/0.72	0.62/0.59
Heat transfer coeff., $W \cdot m^{-2} \cdot K^{-1}$	/107	/104	/106	/107	/102

Table 8. Heterogeneity of the Reactor Model

Operating Conditions		Exp.	Pred.
Feed rate = 1.68 $m^3 \cdot h^{-1}$	Hot-spot temp.	440°C	451°C
Salt-bath temp. = 400°C	Conversion	90%	90.8%
Inlet butane = 1.82%	Selectivity	60%	58%

Reactor Location m	Temperature, °C			Effectiveness Factor			Selectivity	CO/CO_2
	Avg.	Axial	Pellet Surface	η_1	η_2	η_3		
0.2	411.5	415.0	413.3	0.62	2.80	0.98	77.1	1.20
0.4	436.5	447.7	439.1	0.66	1.72	0.95	71.9	1.34
0.6	438.2	447.9	440.6	0.72	1.38	0.94	68.8	1.45
1.0	423.9	431.2	425.3	0.82	1.15	0.95	65.8	1.51
2.0	412.4	416.2	413.1	0.89	1.06	0.95	62.4	1.56
4.0	406.1	408.0	406.5	0.90	1.02	0.92	58.8	1.65

The heterogeneity of the model is illustrated from data with a fresh catalyst at a salt temperature of 400°C. Table 8 shows that in the hot-spot region, the pellet surface is about 2-3°C higher than the average gas temperature. Intraparticle temperature gradients are negligible. By assuming a parabolic radial temperature profile, it is possible to estimate that, in the hot-spot region, the average gas temperature in the tube cross-section is about 11°C lower than the axial value predicted by the model.

Figure 4 illustrates the region of stable operation in contrast to runaway, with feed rate as a parameter. The development of more active and selective catalysts would allow inlet butane concentrations of 4-5% to be used in stable operation in axial-flow fixed-bed reactors.

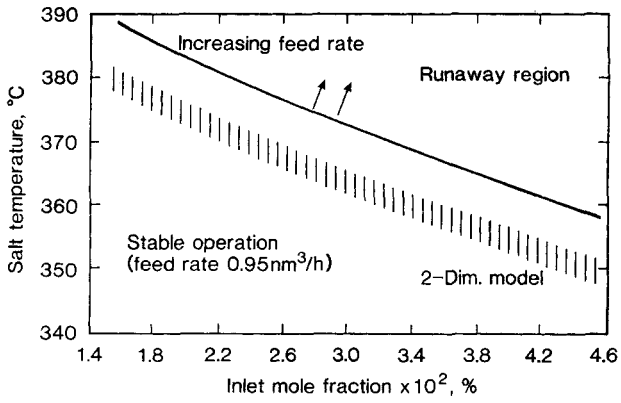

Figure 4. Region of 'STABLE' operation.

Acknowledgment

One of the authors (RKS) acknowledges financial support from KWF Bern, ETH Zurich and Swiss Aluminium, Neuhausen. The reactor work was performed by Dr. J. P. Stringaro, Messrs. M. Bollinger and H. P. Keller in Neuhausen. This article was presented in preliminary form at the AIChE Meeting in San Francisco, November 1984, the delay in publication being a requirement of a confidentiality agreement.

Notation

a_{ij} = number of moles of species i involved in reaction j
A = reactor surface area/reactor volume, m^{-1}
b = half thickness of the active phase in the pellet, m
C_i = concentration of species i, $mol \cdot m^{-3}$
C_p = specific heat of the gas, $J \cdot kg^{-1} \cdot K^{-1}$
dp = diameter of sphere of equal volume to surface area, m
D_{ax} = axial dispersion coefficient, $m^2 \cdot s^{-1}$
D_{effi} = effective diffusivity of species i, $m^2 \cdot s^{-1}$
E_j = activation energy of reaction step j, $J \cdot mol^{-1}$
E_p = catalyst particle porosity
F_t = total gas molar flow rate, $mol \cdot s^{-1}$
G_m = gas mass velocity, $kg \cdot m^{-2} \cdot s^{-1}$
$h_{w,eff}$ = apparent wall heat transfer coefficient, $W \cdot m^2 \cdot K^{-1}$
$-\Delta H_j$ = heat of reaction of step j, $J \cdot mol^{-1}$
kg, h = interphase mass and heat transfer coefficient, $m \cdot s^{-1}$ and $W \cdot m^{-2} \cdot K^{-1}$
k_{gs} = molecular conductivity of air, $W \cdot m^{-1} \cdot K^{-1}$
k_j = rate constant of step j
$k_{r,eff}$ = effective radial thermal conductivity of the bed, $W \cdot m^{-1} \cdot K^{-1}$
K_{eff} = effective thermal diffusivity of the catalyst pellet, $W \cdot m^{-1} \cdot K^{-1}$
K_2 = maleic anhydride adsorption rate constant, atm^{-1}
M = molecular weight
n, p = number of moles of oxygen required/mole of reactant
Pe_p = Peclet number of axial dispersion (udp/Dax)
p_i = mole fraction of species i in the mixture
Pr, Sc = Prandtl and Schmidt number for the gas
R = universal gas constant, $J \cdot mol^{-1} \cdot K^{-1}$
r = distance from pellet center to any point inside the pellet, m
$R(j)$ = intrinsic reaction rate of j, $mol \cdot s^{-1} \cdot m^{-3}$
Re_p = Reynolds number ($G_m dp/\mu$)
S = objective function defined in Eq. 25
T, P = temperature and pressure, K and atm
U_{ov} = overall heat transfer coefficient, $W \cdot m^{-2} \cdot K^{-1}$
u = linear gas velocity, $m \cdot s^{-1}$
Z = distance from reactor inlet, m

Greek letters

ρ = gas density, $kg \cdot m^{-3}$
$\eta(j)$ = effectiveness factor for step j
ϵ = catalyst bed voidage
μ = gas viscosity, $kg \cdot m^{-1} \cdot s^{-1}$
τ = catalyst tortuosity factor
$\alpha(j)$ = exponent in rate equation for step j
Ω = cross-sectional area of reactor tube, m^2

Subscripts

1, 2, 3, 4 = butane, maleic anhydride, CO_2, CO
K, B = Knudsen, bulk
G, MA = gas, maleic anhydride
o, p = bulk gas or reactor inlet, particle
s, t = salt, tube

Literature Cited

Buchanan, J. S., private communication (Mar. 1985).

Budi, F., A. Neri, and G. Stefani, "Future MA Keys to Butane," *Hydro. Proc.*, 159 (Jan. 1982).

Centi, G., F. Trifiro, J. R. Ebner, and V. M. Franchetti, "Mechanistic Aspects of Maleic Anhydride Synthesis from C_4 Hydrocarbons over Phosphorus Vanadium Oxide," *Chem. Rev.*, **88**, 55 (1988).

Contractor, R. M., H. E. Bergna, H. S. Horowitz, C. M. Blackstone, U. Chowdhry, and A. W. Sleight, "Butane Oxidation to Maleic Anhydride in a Recirculating Solids Reactor," *Catalysis 1987*, 647, J. W. Ward, ed., Elsevier, Amsterdam (1988).

Cresswell, D. L., and N. H. Orr, "Measurement of Binary Gaseous Diffusion Coefficients within Porous Catalysts," *Residence Time Distribution Theory*, G. Petha and R. D. Nobel, eds., Verlag Chemie GmbH, D-6940 Weinheim, 41 (1982).

Cropley, J. B., "Systematic Errors in Recycle Reactor Kinetic Studies," *Chem. Eng. Prog.*, **83**, 46 (1987).

De Maio, D. A., "Will Butane Replace Benzene As a Feedstock for Maleic Anhydride?" *Chem. Eng.*, 104, (May 19, 1980).

Dwivedi, P. N., and S. N. Upadhyay, "Particle-Fluid Mass Transfer in Fixed and Fluidized Beds," *Ind. Eng. Chem. Proc. Des. Dev.*, **16**, 157 (1977).

Ergun, S., "Fluid Flow through Packed Columns," *Chem. Eng. Prog.*, **48**, 89 (1952).

Escardino, A., C. Sola, and F. Ruiz, *Ind. Eng. Chem. Prod. Res. Dev.*, **18**, 7 (1979).

Froment, G. F., "Fixed-Bed Reactors—Steady-State Conditions," *Proc. Int. Sym. Chem. Reaction Eng.*, Elsevier, Amsterdam (1972).

Gunn, D. J., "Transfer of Heat or Mass to Particles in Fixed and Fluidized Beds," *Int. J. Heat and Mass Transfer*, **21**, 467 (1978).

Hodnett, B. K., "An Overview of Recent Developments in Elucidating the Mechanism of Selective Oxidation of C-4 Hydrocarbons over Vanadium Phosphorus Oxide Catalysts," *Cat. Today*, **1**, 527 (1987).

Klaus, R., and D. W. T. Rippin, "A New Flexible and Easy to Use General Purpose Regression Program for Handling a Variety of Single and Multiresponse Situations," *Comp. and Chem. Eng.*, **3**, 105 (1979).

Kuhn, P., "Maleic Anhydride Decomposition," internal report, Alusuisse (1979).

Malow, M., "Benzene or Butane for MAN," *Hydro. Processing*, 149 (Nov., 1980).

Neri, A., and S. Sanchioni, US 4.314.946 to Ftalital S. p. A., "Process for the Continuous Separation of Maleic Anhydride from Process Gases," (Feb. 9, 1982).

Perry, R. H., C. H. Chilton, and S. D. Kirkpatrick, *Chemical Engineers' Handbook*, 4th ed., McGraw Hill, New York, 9 (1963).

Satterfield, C. N., "Mass Transfer in Heterogeneous Catalysis," Chap. 1, MIT Press, Cambridge, MA (1970).

Schaffel, G. S., S. S. Chen and J. J. Graham, "Maleic Anhydride from Butane-Catalytic Oxidation in a Fluidized Bed," *Erdoel und Kohle*, Bd. 36, Heft 2, 85 (1983).

Schneider, P., G. Emig, and H. Hofmann, "Kinetic Investigation and Reactor Simulation for the Catalytic Gas-Phase Oxidation of *n*-Butane to Maleic Anhydride," *Ind. Eng. Chem. Res.*, **26**, 2236 (1987).

Seinfeld, J. H., and L. Lapidus, "Process Modelling, Estimation and Identification," Vol. 3, *Mathematical Methods in Chemical Engineering*, Prentice Hall (1974).

Sharma, R. K., D. L. Cresswell, and E. J. Newson, "Selective Oxidation of Benzene to Maleic Anhydride at Commercially Relevant Conditions," *Int. Chem. Eng. Symp. Ser.*, No. 87, Edinburgh (Sept., 1984a).

Sharma, R. K., D. L. Cresswell, and E. J. Newson, "Kinetics and Reactor Modeling in Fixed-Bed Pilot-Plant Production of Maleic Anhydride by the Oxidation of *n*-Butane," AIChE Meeting, San Francisco, paper 69b (Nov. 1984b).

Villadsen, J., and M. L. Michelsen, *Solution of Differential Equation Models by Polynomial Approximation*, Prentice Hall (1978).

Wellauer, T., D. L. Cresswell, and E. J. Newson, "Heat Transfer in Packed Reactor Tubes Suitable for Selective Oxidation," *ACS Symp. Ser.*, **196**, 527 (1982).

Wellauer, T., D. L. Cresswell, and E. J. Newson, "Optimal Policies in Maleic Anhydride Production through Detailed Reactor Modeling," *Chem. Eng. Sci.*, **41**, 765 (1986).

Wenig, R. W., and G. L. Schrader, "*In Situ* FTIR Study of *n*-Butane Selective Oxidation to Maleic Anhydride on V-P-O Catalysts," *J. Phys. Chem.*, **90**, 6480 (1986).

Manuscript received Sept. 11, 1989, and revision received Nov. 5, 1990.